Citation: CPT Pharmacometrics Syst. Pharmacol. (2014) 3, e147; doi:10.1038/psp.2014.46

www.nature.com/psp

ORIGINAL ARTICLE

# Linking the Population Pharmacokinetics of Tenofovir and Its Metabolites With Its Cellular Uptake and Metabolism

K Madrasi[1], RN Burns[2], CW Hendrix[3], MJ Fossler[4] and A Chaturvedula[1]

**Empirical pharmacokinetic models are used to explain the pharmacokinetics of the antiviral drug tenofovir (TFV) and its metabolite TFV diphosphate (TFV-DP) in peripheral blood mononuclear cells. These empirical models lack the ability to explain differences between the disposition of TFV-DP in HIV-infected patients vs. healthy individuals. Such differences may lie in the mechanisms of TFV transport and phosphorylation. Therefore, we developed an exploratory model based on mechanistic mass transport principles and enzyme kinetics to examine the uptake and phosphorylation kinetics of TFV. TFV-DP median $C_{max}$ from the model was 38.5 fmol/$10^6$ cells, which is bracketed by two reported healthy volunteer studies (38 and 51 fmol/$10^6$ cells). The model presented provides a foundation for exploration of TFV uptake and phosphorylation kinetics for various routes of TFV administration and can be updated as more is known on actual mechanisms of cellular transport of TFV.**
*CPT Pharmacometrics Syst. Pharmacol.* (2014) **3**, e147; doi:10.1038/psp.2014.46; published online 12 November 2014

Tenofovir disoproxil fumarate (TDF) is an ester prodrug of tenofovir (TFV) and has US Food and Drug Administration approval for the indications of human immunodeficiency virus (HIV) treatment and prevention. After oral administration, TDF is rapidly converted by esterases[1] in plasma to TFV, which is an analog of the endogenous deoxyadenosine monophosphate. TFV is the predominant circulating form[2,3] which can then be taken up by cells normally targeted by HIV for infection ($CD4^+$ lymphocytes). Subsequently, TFV undergoes two phosphorylation steps forming tenofovir diphosphate (TFV-DP), which is an analog of endogenous deoxyadenosine triphosphate. TFV-DP competes with deoxyadenosine triphosphate for incorporation into viral DNA by HIV-1 reverse transcriptase, which then prevents further DNA polymerization once TFV-DP gets incorporated.[4] TFV-DP thus can slow down or inhibit the production of proviral DNA, which is essential for host cell infection and viral replication.

Understanding the clinical pharmacology of the active moiety, TFV-DP, is essential to optimize clinical outcomes. Several empirical pharmacokinetic models are currently used to explain the pharmacokinetics of TFV and TFV-DP after oral administration of TDF.[2,5,6] Most studies have only characterized the pharmacokinetics of TFV[2,7–10] but some recent studies have also focused on intracellular kinetics of the active anabolite TFV-DP.[6,11–14] In these studies, the parameters concerning the process of TFV uptake to TFV-DP formation are lumped. The role of the underlying mechanistic aspects of TFV uptake by immunological cells, including intracellular TFV phosphorylation and possible TFV efflux mechanisms, which may determine the pharmacokinetics of TFV-DP in the intracellular space were unexplored according to publicly available data. Thus, there is scope for a mathematical model that can explore mechanisms of TFV uptake and phosphorylation and act as a hypothesis generator for future experiments and models.

Such a mathematical model will require translating findings of basic research toward the goal of simulating clinical outcomes. These findings are generally obtained during preclinical experimentation on enzyme kinetics of drug metabolic reactions and drug transporters prior to the design of clinical trials. However, it was not an established practice until very recently to use such experimental data in predicting phase I clinical studies other than allometric scaling.[15–17] Biological drug development has only recently evolved to using such *in vitro* data to support first-in-human dose calculations by minimally anticipated biological effect levels concepts.[18] Other recent developments include model-based drug development where mathematical models with varied complexity are developed depending on the stage of development,[19,20] physiologically based pharmacokinetic modeling[21,22] and systems based modeling where models account for complex biology and pharmacology. These new approaches to drug development are very useful for predicting pharmacokinetic outcomes in early phase clinical studies where models can provide rational clinical trial designs.

The objective of this analysis was to develop an integrated pharmacokinetic model to account for passive diffusion, a saturable channel-based uptake, MRP4 channel-based efflux, and TFV phosphorylation through kinases using published parameters values. TFV-MP and TFV-DP kinetic profiles in the peripheral blood mononuclear cell (PBMC) compartment were simulated. Finally, the model was taken to the population level in order to compare the predictions to the available clinical data.

## RESULTS

### Mathematical model of TFV transport to PBMCs

The model used for simulating TFV uptake and conversion to TFV-DP is shown in **Figure 1**. A two-compartment pharmacokinetic model with a dosing compartment[6] was used

[1]Department of Pharmacy Practice, Mercer University, Atlanta, Georgia, USA; [2]Department of Pharmaceutical Sciences, Mercer University, Atlanta, Georgia, USA; [3]Division of Clinical Pharmacology, John Hopkins University, Baltimore, Maryland, USA; [4]Clinical Pharmacology Modeling and Simulation, GlaxoSmithKline, King of Prussia, Pennsylvania, USA. Correspondence: K Madrasi (kumpal.madrasi@gmail.com)
Received 11 June 2014; accepted 3 September 2014; published online 12 November 2014. doi:10.1038/psp.2014.46

to describe the plasma concentration profile of TFV after oral administration of TDF. Simulations were done for TFV uptake to the PBMCs through diffusion and a saturable transport channel and TFV efflux through MRP4-based activity. Assumptions used in the model and defining equations have been described in the **Supplementary Material**.

### Model testing and validation

The mechanistic model developed was used for simulating pharmacokinetic profiles after oral administration of TDF. Initial testing of the model was done through single and multidose simulations for TDF doses of 75, 150, 300, and 600 mg. Single-dose simulations were performed with a time span of 240 h and multidose simulations were performed with a time span of 480 h. Concentration–time courses for plasma TFV, PBMC TFV-MP, and PBMC TFV-DP were plotted. The model that achieved saturation was validated with data from the oral substudy of the MTN-001 trial[23] by a simulation of a population of 100 subjects assumed to be fully adherent. Between subject variability was added from literature[11] on the pharmacokinetic model of TFV with saturable uptake and no variability was assumed on the TFV uptake and metabolism components of the model.

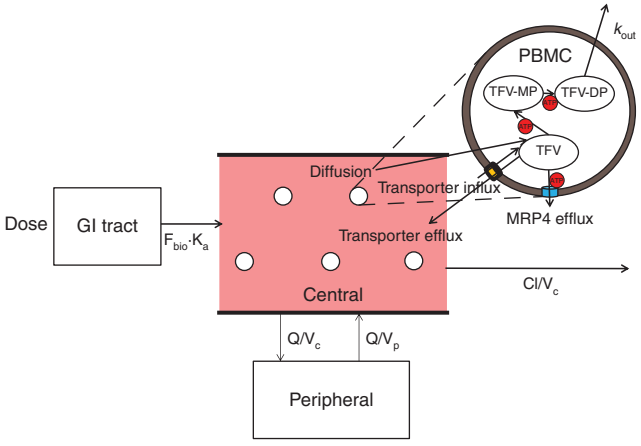


**Figure 1** Model schematic for simulating TFV pharmacokinetics, tenofovir (TFV) uptake at peripheral blood mononuclear cell (PBMC), and TFV-DP formation. $F_{bio}$ indicates bioavailability of the drug, $K_a$ is the absorption constant, $Q$ is the intercompartmental clearance, $V_c$ is the central compartment volume, $V_p$ is the peripheral compartment volume, Cl is the clearance of TFV, and $k_{out}$ is the elimination of TFV-DP.

### Impact of diffusion on TFV uptake at PBMC level

**Figure 2** and **Supplementary Figure S1 a–c** indicate single- and multidose simulations of Plasma TFV, PBMC TFV, and PBMC TFV-DP levels at TDF doses of 75–600 mg with the model containing diffusion and channel mediated uptake. **Figure 3** and **Supplementary Figure S2 a–c** (refer supplement) show the same for a model containing only channel mediated uptake. No difference was observed between the two scenarios. Hence, diffusion based uptake of TFV will be neglected in the final model to come to a mathematically simpler model.

### Model with saturable TFV uptake

**Figure 4** and **Supplementary Figure S3 a–c** indicate single- and multidose simulations of plasma TFV, PBMC TFV-MP, and PBMC TFV-DP levels at TDF doses of 75–600 mg with the model containing a lower $K_m$ and a higher $k_{leak}$ across the PBMC. A saturating behavior appears immediately at a TDF dose of above 75 mg and gets more prominent at higher TDF doses. The simulations for the single dose give a plasma TFV $t_{max}$ of 2 h as predicted before.[6] The single-dose simulations of TDF dose at 300 mg reveal a TFV-DP peak of 11.35 fmol/$10^6$ cells and the multidose simulations reveal an end TFV-DP amount of 35 fmol/$10^6$ cells.

### Model validation

**Figure 5a–d** shows the outcome of adding interindividual variability to the model. **Figure 5a,b** indicates the 5, 50, and 95 percentile values of day 1 of the multiple dosing regimen; **Figure 5c,d** indicates the same for day 14. Steady-state TFV and TFV-DP readings from the MTN-001 study are added in **Figure 5c,d** respectively.

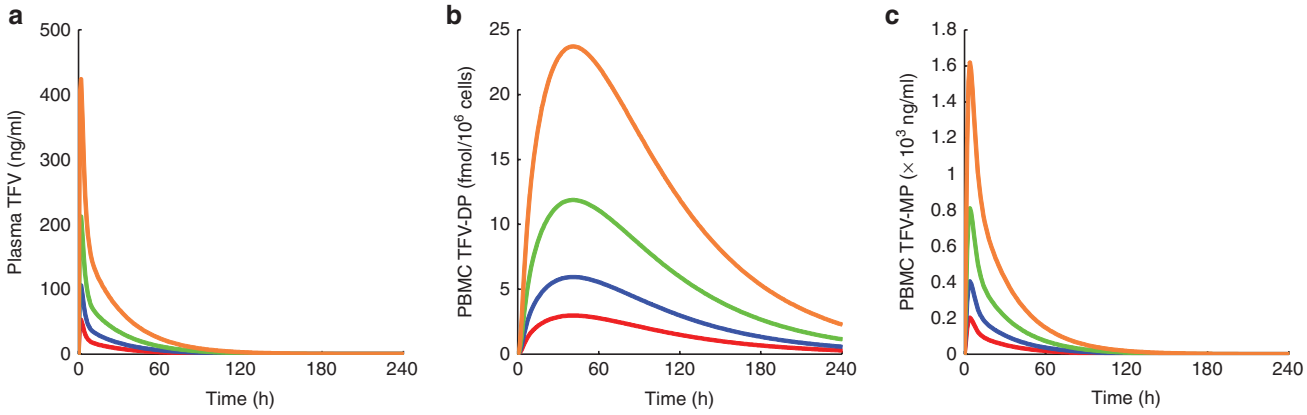


**Figure 2** Single-dose simulations of diffusion and channel-mediated transport working in parallel. Red line indicates a tenofovir (TFV) disoproxil fumarate (TDF) dose of 75 mg, blue line indicates a dose of 150 mg, green line indicates a dose of 300 mg, and the orange line indicates a dose of 600 mg. (**a**) TFV concentrations in plasma, (**b**) TFV-DP concentrations in peripheral blood mononuclear cells (PBMCs), (**c**) TFV-MP concentrations in PBMCs.

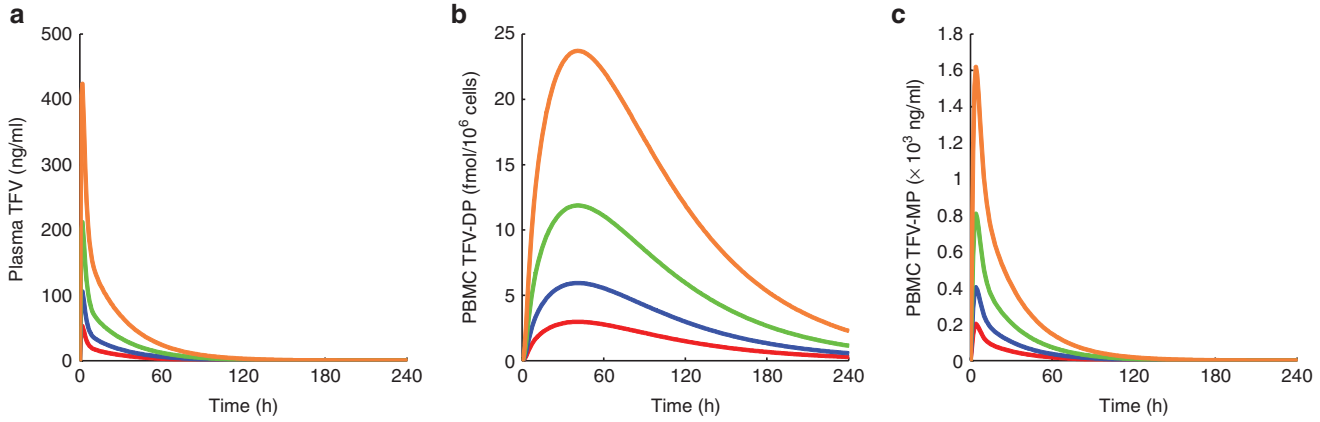


**Figure 3** Single-dose simulations of channel mediated transport. Red line indicates a tenofovir (TFV) disoproxil fumarate (TDF) dose of 75 mg, blue line indicates a dose of 150 mg, green line indicates a dose of 300 mg, and the orange line indicates a dose of 600 mg. (**a**) TFV concentrations in plasma, (**b**) TFV-DP concentrations in peripheral blood mononuclear cells (PBMCs), (**c**) TFV-MP concentrations in PBMCs.

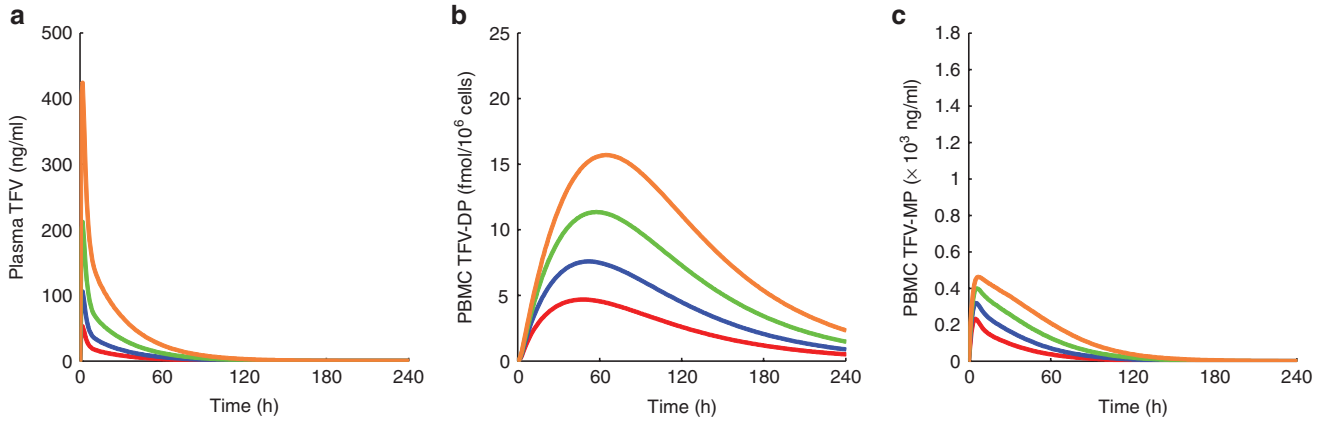


**Figure 4** Single-dose simulations of the saturation model. Red line indicates a tenofovir (TFV) disoproxil fumarate (TDF) dose of 75 mg, blue line indicates a dose of 150 mg, green line indicates a dose of 300 mg, and the orange line indicates a dose of 600 mg. (**a**) TFV concentrations in plasma, (**b**) TFV-DP concentrations in peripheral blood mononuclear cells (PBMCs), (**c**) TFV-MP concentrations in PBMCs.

### Sensitivity analysis

**Supplementary Figure S4** shows the 50 different model responses obtained from the different combinations of parameters tested. **Table 1** depicts the sensitivity indices obtained from the sensitivity analysis. The efflux of TFV from MRP4 ($k_{leak}$), enzyme concentration ($E_1$) of human adenylate kinase 2 (hAK2), hAK2 turnover number ($k_{cat1}$), the Michaelis–Menten constant for TFV monophosphorylation ($K_{m1}$) showed statistically significant indices for all of the outputs. Positive indices were obtained for $k_{cat1}$ and $E_1$, while negative indices were obtained for $k_{leak}$ and $K_{m1}$. The negative coefficients suggest that as the respective parameters increase, the outputs decrease, while positive coefficients suggest the opposite.

## DISCUSSION

TFV and other nucleoside reverse transcriptase inhibitors are known to exert their effects through their intracellular metabolite thus examining the process of nucleoside reverse transcriptase inhibitor phosphorylation in detail is important to their pharmacological effect. In the model described, a two-compartment model was used to explain the pharmacokinetics of TFV, while the uptake of TFV by PBMCs and subsequent phosphorylation was analyzed in greater detail. Saturable uptake/metabolism was previously modeled by other authors.[6,11] Duwal *et al.*[6] had estimated a $K_m$ of 29 ng/ml for TFV-DP formation by coupling PK model with mechanistic viral dynamics model and reproduced the efficacy curves of TFV monotherapy. The steady-state trough concentrations reported after 300 mg QD and 600 mg QD dosing were 64 and 111 ng/ml respectively.[24] Since the estimated $K_m$ value is much lower than the trough concentrations, the uptake for TFV should be nearly saturated at 300 and 600 mg QD dosing. So, we focused our simulations toward capturing the saturation phenomenon. Three possible models for TFV uptake were analyzed: (i) a model where diffusion and a saturable transporter are responsible, (ii) another where only the saturable transporter is responsible, and (iii) a third model which we propose as a way to explain saturable TFV uptake. It was found that under the current parameters selected, diffusion should not play a major role in TFV uptake. This is in agreement with the poor permeability of TFV through physiological membranes due to its negative charge. This led to the development of the prodrug TDF to improve

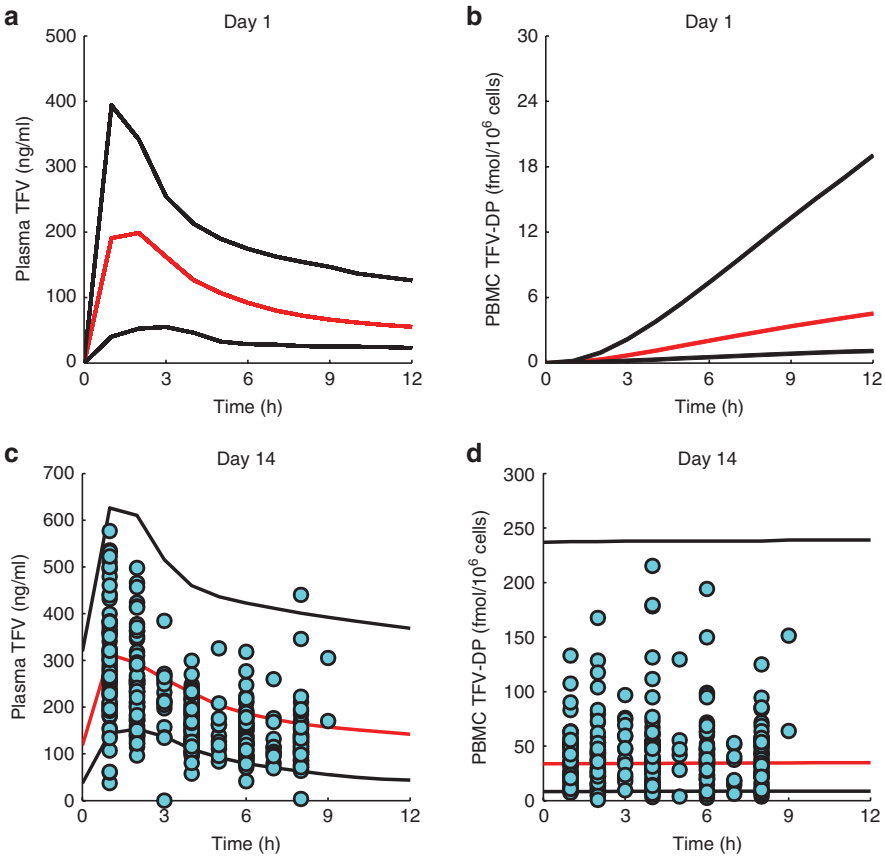


**Figure 5** Visual predictive check for validating model. Black lines indicate 5 and 95 percentile values and red line indicates median. Cyan markers indicate observed data from MTN-001 study. (**a**) Plasma tenofovir (TFV) concentrations from the simulations on day 1, (**b**) peripheral blood mononuclear cell (PBMC) TFV-DP amounts from the simulations, (**c**) plasma TFV concentrations from the simulations on day 14 (steady state), (**d**) PBMC TFV-DP amounts from the simulations.

TFV bioavailability, yet the reported absolute bioavailability of TFV is in the range of 0.25–0.32. Moreover, the minimal role of diffusion should be an expected feature if TFV uptake is considered saturable. A prominent role of diffusion would have made TFV uptake proportional to the dose and saturation would not have been observed. TFV diffusion might also be precluded due to much of TFV being in the ionized form at the pH level of blood (pKa1 = 3.8 and pKa2 = 6.7 for TFV[25]; pH of blood = 7.4)

The model with saturable TFV uptake was simulated for a population of 100 subjects with interindividual variability on pharmacokinetic parameters derived from an earlier work.[11] A visual predictive check of the simulations revealed a good match with data from the MTN-001 study.[23] TFV-DP accumulates slowly owing to its long half-life of (48 h in this model).[26] We predict that the model will reach steady state in 14 once daily dosing events. Our model predicted individual TFV-DP amount in the range of 4.715 to 139.5 fmol/$10^6$ cells and a median of 38.5 fmol/$10^6$ cells which covers the range of most data points from the MTN-001 study. The comparable median $C_{max}$ from the MTN-001 study is 51 fmol/$10^6$ cells,[23] which our model came close to. Some accuracy is lost for the lower side of population variability, however that is expected since in our simulations, the 100 subjects have 100% adherence but in the MTN-001 trial, only 64% subjects were expected to be perfectly adherent.[27]

**Table 1** Least squares estimates of sensitivity coefficients $\beta_{i,j}$

| | | Model output | | |
|---|---|---|---|---|
| | Uncertainty | $C_{max}$ (fmol/$10^6$ cells) | $C_{tr}$ (fmol/$10^6$ cells) | AUC |
| Parameter | (±%) | $\beta_{i,j}$ (%/%) | $\beta_{i,j}$ (%/%) | $\beta_{i,j}$ (%/%) |
| $k_{cat1}$ | 10 | **1.4056** | **1.3987** | **1.4604** |
| $k_{cat2}$ | 10 | –1.9050 | –1.8931 | –2.0181 |
| $K_{m1}$ | 10 | **–0.4518** | **–0.3712** | **–0.5139** |
| $K_{m2}$ | 10 | –0.3986 | –0.4790 | –0.4290 |
| $E_1$ | 20 | **1.3428** | **1.3413** | **1.3724** |
| $E_2$ | 20 | 0.1244 | 0.2004 | 0.1372 |
| $k_{leak}$ | 10 | **–1.1626** | **–1.1566** | **–1.2002** |
| $V_{max}$ | 10 | 0.9037 | 0.8924 | 0.9126 |
| $K_m$ | 10 | –0.4342 | –0.2879 | –0.4520 |
| $k_{out}$ | 15 | –0.023 | 0.2354 | –0.3777 |

Statistically significant coefficients are in boldface.

To understand what factors the model is the most sensitive to, we conducted sensitivity analysis. The highest relative sensitivity indices were obtained in parameters related to TFV efflux through MRP4 and the monophosphorylation step, thus suggesting that the model is sensitive to these parameters. Ascertaining the details of TFV function in PBMCs would thus require experimentation on these parameters. Differences in these parameters may

**Table 2** Uncertainty for input parameters in the model

| Parameter | Description | Uncertainty |
|---|---|---|
| $k_{cat1}$ | Turnover number for AK2 and TFV | ±10% |
| $K_{m1}$ | Michaelis-Menten constant for AK2 and TFV | ±10% |
| $k_{cat2}$ | Turnover number for NDKA and TFV-MP | ±10% |
| $K_{m2}$ | Michaelis-Menten constant for NDKA and TFV-MP | ±10% |
| $E_1$ | Enzyme concentration for hAK2 | ±20% |
| $E_2$ | Enzyme concentration for NDKA | ±20% |
| $k_{leak}$ | Leakage of TFV from cells | ±10% |
| $V_{max}$ | Maximum rate of TFV uptake through OATP3A1 | ±10% |
| $K_m$ | Michaelis-Menten of OATP3A1 for TFV | ±10% |
| $k_{out}$ | Elimination of TFV-DP from PBMC | ±15% |

PBMC, peripheral blood mononuclear cell; TFV, tenofovir.

also reveal how TFV-DP levels in infected and healthy individuals may be different. The median TFV-DP $C_{max}$ for infected individuals has been reported to range from 89.9 to 120 fmol/$10^6$ cells,[13,28] much higher than for reports in healthy individuals which range from 38 fmol/$10^6$ cells in a directly observed daily dosing study[29] and 51 fmol/$10^6$ cells in MTN-001.[23]

There are competing hypotheses for TFV transport in PBMCs such as a transporter-mediated process and/or endocytosis.[6,30,31] There is also a dearth of experimental data on types and concentrations of kinases involved in the phosphorylation process. Thus, the model should be further updated to account for future findings. In the future, we will also attempt to extend the model by incorporating viral dynamics and using drug adherence pattern simulation strategies to understand probable efficacy of treatment in patients. It has been suggested that the drug adherence can become a major obstacle for the success of a drug.[32] If poor drug adherence can be predicted through simulations after a trial run, then sufficient intervention may be attempted using appropriate technological means to improve adherence. The mechanistic model may be of use at this point to calculate threshold adherence, below which the drug will fail. Calculation of such a threshold adherence will provide a useful benchmark to make necessary interventions to improve adherence.

In conclusion, we created a template for the modeling of current and future anti-retroviral drugs in various target sites. Experimentation requirements as suggested for TFV through simulations and subsequent sensitivity analysis might also be performed for them. Using such models, it might also be possible to study and provide an explanation for low penetration of antiretroviral drugs in certain organs like testes and the brain.[33,34]

## METHODS

### Model validation

All the differential equations for the single-dose and multi-dose simulations were implemented using the ODE15s solver in MATLAB R2013a (MathWorks, Natick, MA). For population simulations, a population of 100 subjects was simulated for multiple TDF doses of 300 mg taken at every 24 h for a period of 14 days with 100% adherence. Simulations were conducted in NONMEM 7.2 (Icon, Ellicott City, MD) using ADVAN8 subroutine. 5, 50 and 95 percentile values of plasma TFV and PBMC TFV-DP at steady state were calculated from the simulations and were compared against data from MTN-001 trial which included an arm with daily oral TDF dosing for 6 weeks, with PK sampling done in plasma and PBMC for 8 h.

### Uncertainty and sensitivity analyses

Perturbation of model parameters was performed to identify the input parameters that have the most impact on the outputs. A Latin Hypercube Sampling method was chosen for sampling parameter space based on a comparison of sampling techniques,[35] and sensitivity analysis reported earlier.[36,37]

The model scenario selected for the sensitivity analysis was the one which simulated a saturable TFV uptake. Output parameters chosen were maximum TFV-DP amount in the PBMC compartment ($C_{max}$), TFV-DP amount at 24 h ($C_{tr}$) and AUC for TFV-DP concentrations. Each parameter was divided into 50 equal probability density regions based on their uncertainty. Fifty simulation runs were performed with the parameters chosen randomly and without repetition from the possible values. To examine the sensitivity between the output concentrations and the input parameters, the sensitivity indices were determined from linear least squares multiple regression applied to the following relationship:

$$Y_i^k = \beta_{i,0} + \beta_{i,1}X_1^k + \beta_{i,2}X_2^k + \ldots\ldots + \beta_{i,j}X_j^k \quad (1)$$

where $i$ is the number of the output parameter and $j$ is the number of the input parameter. $Y_i^k$ is the change in % of the $i^{th}$ output at the $k^{th}$ run from the $i^{th}$ output derived by the initial estimates of the parameters and $X_j^k$ is a change in % of the central value of the $j^{th}$ parameter. Confidence intervals for the sensitivity indices were calculated using the "regress" function in Matlab. If the confidence interval did not include zero, then the respective sensitivity index $\beta_{i,j}$ can be said to significantly impact the output. Input parameters were assigned uncertainty ranges (**Table 2**) based on the confidence in the reported central values, quality of the fits and the ability to determine importance of parameters.

**Acknowledgments.** This publication was supported by a sub-agreement from The Johns Hopkins University, School of Medicine. Its contents are solely the responsibility of the authors and do not necessarily represent the official views of The Johns Hopkins University, School of Medicine.

**Author Contributions.** K.M. wrote the manuscript. A.C. designed the research. K.M. performed the research. R.N.B., C.W.H., M.F., and A.C. analyzed the data.

**Conflict of Interest.** The authors declared no conflict of interest.

## Study Highlights

### WHAT IS THE CURRENT KNOWLEDGE ON THE TOPIC?

✓ Conventionally, TFV-DP pharmacokinetics are simulated with lumped parameters which take into account only the overall process of TFV-DP formation in PBMCs. Details of this process are overlooked.

### WHAT QUESTION DID THIS STUDY ADDRESS?

✓ The study proposes a mechanistic model to analyze TFV-DP formation given TFV pharmacokinetics.

### WHAT THIS STUDY ADDS TO OUR KNOWLEDGE

✓ The study attempts to incorporate TFV mono- and diphosphokinases as well as TFV transport channel activities in the process of TFV-DP formation.

### HOW THIS MIGHT CHANGE CLINICAL PHARMACOLOGY AND THERAPEUTICS

✓ Different TFV-DP levels have been found in healthy and infected individuals.[13,23] Approaches in mechanistic modeling of TFV transport and TFV-DP formation may allow for identification of elements that cause such changes. It is our hope that identification of underlying physiology of TFV transport and TFV-DP formation may lead to better treatment or prophylactic regimes.

1. Anderson, P.L., Kiser, J.J., Gardner, E.M., Rower, J.E., Meditz, A. & Grant, R.M. Pharmacological considerations for tenofovir and emtricitabine to prevent HIV infection. *J. Antimicrob. Chemother.* **66**, 240–250 (2011).
2. Kearney, B.P., Flaherty, J.F. & Shah, J. Tenofovir disoproxil fumarate: clinical pharmacology and pharmacokinetics. *Clin. Pharmacokinet.* **43**, 595–612 (2004).
3. Naesens, L., Balzarini, J., Bischofberger, N. & De Clercq, E. Antiretroviral activity and pharmacokinetics in mice of oral bis(pivaloyloxymethyl)-9-(2-phosphonylmethoxyethyl) adenine, the bis(pivaloyloxymethyl) ester prodrug of 9-(2-phosphonylmethoxyethyl) adenine. *Antimicrob. Agents Chemother.* **40**, 22–28 (1996).
4. von Kleist, M., Metzner, P., Marquet, R. & Schütte, C. HIV-1 polymerase inhibition by nucleoside analogs: cellular- and kinetic parameters of efficacy, susceptibility and resistance selection. *PLoS Comput. Biol.* **8**, e1002359 (2012).
5. Dixit, N.M. & Perelson, A.S. Complex patterns of viral load decay under antiretroviral therapy: influence of pharmacokinetics and intracellular delay. *J. Theor. Biol.* **226**, 95–109 (2004).
6. Duwal, S., Schütte, C. & von Kleist, M. Pharmacokinetics and pharmacodynamics of the reverse transcriptase inhibitor tenofovir and prophylactic efficacy against HIV-1 infection. *PLoS One* **7**, e40382 (2012).
7. Blum, M.R., Chittick, G.E., Begley, J.A. & Zong, J. Steady-state pharmacokinetics of emtricitabine and tenofovir disoproxil fumarate administered alone and in combination in healthy volunteers. *J. Clin. Pharmacol.* **47**, 751–759 (2007).
8. Chittick, G.E. *et al.* Pharmacokinetics of tenofovir disoproxil fumarate and ritonavir-boosted saquinavir mesylate administered alone or in combination at steady state. *Antimicrob. Agents Chemother.* **50**, 1304–1310 (2006).
9. Droste, J.A. *et al.* Pharmacokinetic study of tenofovir disoproxil fumarate combined with rifampin in healthy volunteers. *Antimicrob. Agents Chemother.* **49**, 680–684 (2005).
10. Jullien, V. *et al.* Population pharmacokinetics of tenofovir in human immunodeficiency virus-infected patients taking highly active antiretroviral therapy. *Antimicrob. Agents Chemother.* **49**, 3361–3366 (2005).
11. Baheti, G., Kiser, J.J., Havens, P.L. & Fletcher, C.V. Plasma and intracellular population pharmacokinetic analysis of tenofovir in HIV-1-infected patients. *Antimicrob. Agents Chemother.* **55**, 5294–5299 (2011).
12. Barditch-Crovo, P. *et al.* Phase i/ii trial of the pharmacokinetics, safety, and antiretroviral activity of tenofovir disoproxil fumarate in human immunodeficiency virus-infected adults. *Antimicrob. Agents Chemother.* **45**, 2733–2739 (2001).
13. Hawkins, T., Veikley, W., St Claire, R.L. 3rd, Guyer, B., Clark, N. & Kearney, B.P. Intracellular pharmacokinetics of tenofovir diphosphate, carbovir triphosphate, and lamivudine triphosphate in patients receiving triple-nucleoside regimens. *J. Acquir. Immune Defic. Syndr.* **39**, 406–411 (2005).
14. von Kleist, M. & Huisinga, W. Pharmacokinetic-pharmacodynamic relationship of NRTIs and its connection to viral escape: an example based on zidovudine. *Eur. J. Pharm. Sci.* **36**, 532–543 (2009).
15. Huxley, J.S. *Problems of Relative Growth.* BiblioBazaar, 2011.
16. Snell, O. Die Abhängigkeit des Hirngewichtes von dem Körpergewicht und den geistigen Fähigkeiten. *Archiv für Psychiatrie und Nervenkrankheiten* **23**, 436–446 (1892).
17. Thompson, D.A.W. & Bonner, J.T. *On Growth and Form.* Cambridge University Press, New York, 1992.
18. European Medicines Agency, Committee for Medicinal Products for Human Use. *Guideline on Strategies to Identify and Mitigate Risks for First-In-Human Clinical Trials With Investigational Medicinal Products.* European Medicines Agency, London, 2007.
19. Lalonde, R.L. *et al.* Model-based drug development. *Clin. Pharmacol. Ther.* **82**, 21–32 (2007).
20. Milligan, P.A. *et al.* Model-based drug development: a rational approach to efficiently accelerate drug development. *Clin. Pharmacol. Ther.* **93**, 502–514 (2013).
21. Rostami-Hodjegan, A. Physiologically based pharmacokinetics joined with *in vitro-in vivo* extrapolation of ADME: a marriage under the arch of systems pharmacology. *Clin. Pharmacol. Ther.* **92**, 50–61 (2012).
22. Zhao, P. *et al.* Applications of physiologically based pharmacokinetic (PBPK) modeling and simulation during regulatory review. *Clin. Pharmacol. Ther.* **89**, 259–267 (2011).
23. Hendrix, C.W. *et al.* MTN-001: randomized pharmacokinetic cross-over study comparing tenofovir vaginal gel and oral tablets in vaginal tissue and other compartments. *PLoS One* **8**, e55013 (2013).
24. Gilead Sciences Inc. Clinical pharmacology and biopharmaceutics review of Viread. In: *Research.* (Food and Drug Administration, Washington, DC, 2001).
25. Choi, S.U., Bui, T. & Ho, R.J. pH-dependent interactions of indinavir and lipids in nanoparticles and their ability to entrap a solute. *J. Pharm. Sci.* **97**, 931–943 (2008).
26. Louissaint, N.A. *et al.* Single dose pharmacokinetics of oral tenofovir in plasma, peripheral blood mononuclear cells, colonic tissue, and vaginal tissue. *AIDS Res. Hum. Retroviruses* **29**, 1443–1450 (2013).
27. Minnis, A.M. *et al.* Adherence and acceptability in MTN 001: a randomized cross-over trial of daily oral and topical tenofovir for HIV prevention in women. *AIDS Behav.* **17**, 737–747 (2013).
28. Hawkins, T. *et al.* Intracellular nucleotide levels during coadministration of tenofovir disoproxil fumarate and didanosine in HIV-1-infected patients. *Antimicrob. Agents Chemother.* **55**, 1549–1555 (2011).
29. Hendrix, C.W. *et al.* Tenofovir-Emtricitabine Directly Observed Dosing: 100% Adherence Concentrations (HPTN 066). 21st Conference on Retroviruses and Opportunistic Infections, 3–6 March 2014, Boston, MA.
30. Liptrott, N.J., Curley, P., Moss, D., Back, D.J., Khoo, S.H. & Owen, A. Interactions between tenofovir and nevirapine in CD4+ T cells and monocyte-derived macrophages restrict their intracellular accumulation. *J. Antimicrob. Chemother.* **68**, 2545–2549 (2013).
31. Robbins, B.L., Srinivas, R.V., Kim, C., Bischofberger, N. & Fridland, A. Anti-human immunodeficiency virus activity and cellular metabolism of a potential prodrug of the acyclic nucleoside phosphonate 9-R-(2-phosphonomethoxypropyl)adenine (PMPA), Bis(isopropyloxymethylcarbonyl)PMPA. *Antimicrob. Agents Chemother.* **42**, 612–617 (1998).
32. Urquhart, J. Role of patient compliance in clinical pharmacokinetics. A review of recent research. *Clin. Pharmacokinet.* **27**, 202–215 (1994).
33. Kim, A.E., Dintaman, J.M., Waddell, D.S. & Silverman, J.A. Saquinavir, an HIV protease inhibitor, is transported by P-glycoprotein. *J. Pharmacol. Exp. Ther.* **286**, 1439–1445 (1998).
34. Owen, A. *et al. In vitro* synergy and enhanced murine brain penetration of saquinavir coadministered with mefloquine. *J. Pharmacol. Exp. Ther.* **314**, 1202–1209 (2005).
35. McKay, M.D., Beckman, R.J. & Conover, W.J. A comparison of three methods for selecting values of input variables in the analysis of output from a computer code. *Technometrics* **42**, 55–61 (2000).
36. Bui, T.D., Dabdub, D. & George, S.C. Modeling bronchial circulation with application to soluble gas exchange: description and sensitivity analysis. *J. Appl. Physiol. (1985).* **84**, 2070–2088 (1998).
37. Kapela, A., Bezerianos, A. & Tsoukias, N.M. A mathematical model of Ca2+ dynamics in rat mesenteric smooth muscle cell: agonist and NO stimulation. *J. Theor. Biol.* **253**, 238–260 (2008).



Supplementary information accompanies this paper on the *CPT: Pharmacometrics & Systems Pharmacology* website (http://www.nature.com/psp)